

# Maximizing Efficiency of Electromagnetic Resonance Wireless Power Transmission Systems with Adaptive Circuits

Huy Hoang and Franklin Bien

*Ulsan National Institute of Science and Technology  
South Korea*

## 1. Introduction

Wireless power transmission (WPT) is a cutting-edge technology that signifies a new era for electricity without a bunch of wires. Wireless power or wi-power is increasingly becoming the main interest of many R&D firms to eliminate the “last cable” after the wide public exposure of Wi-Fi lately. Even though the first idea was devised from Nikola Tesla in the early 20<sup>th</sup> century (Tesla, 1919), there was never strong demand for it due to the lack of portable electronic devices. In recent years, with the advent of a booming development in cell-phones and mobile devices, the interest of wireless energy has been re-emerged. WPT offers the possibility to supplying power for electronic devices without having to plug them into AC socket. Until now, there have been many efforts to be made to improve this technology as well as its applications. These efforts include medium-range transmission based on electromagnetic resonance and long-range transmission using microwaves (Greene et al., 2007; Brown & Eves, 1992). Although the investigation of long-range power delivery via far-field techniques was carried out with endeavors, the efficiency or power delivery is still quite low that is not sufficient to fully charge typical electronic gadgets overnight. Therefore, increasing the transmitting power is necessary to provide energy enough to consistent DC supply of gadgets. However, the system would be harmful to human according to IEEE standard for radio frequency electromagnetic fields (IEEE, 1999). The other way is to utilize many transmitters simultaneously, but the implementation seems to be impractical. Additionally, the existence of an uninterruptible line of sight (LoS) is mandatory for microwave-based power transmissions and in a case of mobile objects requiring a complicated tracking system. In general, such power transmissions are relatively suited to very low power applications unless they are used in military or space explorations which are less regulated environments. On the other hand, medium-range WPT covering up to 30 feet is a growing research area that finds wide applications. In order to implement a viable WPT system, Q factors of coils and an impedance matching issue are critical and sensitive to achieve a high efficiency. In reality, due to a resonant coupling nature of the system, for the most efficient power transmission, there is an optimum range between a power coil and a transmitting coil for a fixed distance between the transmitting and receiving coils. This effect may not be clarified by a conventional magnetic induction theory. In this chapter, a simple equivalent circuit model for a WPT system via electromagnetic

resonance will be derived and analytically solved. From the solution, above effect could be easily clarified and key concepts including frequency splitting and impedance matching will be mentioned as well. In addition, adaptive circuits, called antenna-locked loops (ALL), are studied to maintain the optimal resonant condition, realize the maximum wireless power transfer efficiency and execute precision resonant frequency optimization by setting the resonant condition with the low Q factor to detect any possible incoming power, then increasing the Q factor while maintaining the resonant condition.

This chapter is organized as follows. In Section 2, Subsection 2.1 introduces a system model and circuit analysis of a four-coil system. Subsection 2.2 describes a comparison of different types of coupling mechanism, while a case of multiple receivers in WPT system is mentioned in Subsection 2.3. Subsection 2.4 shows experimental results. The ideas for ALL systems are presented in Section 3. Finally, Section 4 provides conclusion.

## 2. System model and circuit analysis

The electromagnetic resonance (also called magnetic resonant coupling) WPT based techniques are typically relied on four coils as opposed to two coils used in the conventional inductive links. A typical model of four-coil power transfer system is shown in Fig. 1, which consists of a power coil, a transmitting coil (Tx coil), a receiving coil (Rx coil) and a load coil. The transmitting coil and the receiving coil are also called resonators, which are supposed to resonate at the same frequency. For common cases, sizes of the four coils are different. Indeed, in some applications, the coils in the receiver side are needed to be scaled as small enough to be integrated in portable devices such as laptops, handheld devices or implantable medical equipment. In various cases of practical interest, the receiving and load coils can be fitted within the dimensions of those personal assistant tools, enabling mobility and flexibility properties. Otherwise, it is quite free to determine sizes of the transmitter. Normally, the transmitting coil may be made larger for a higher efficiency of the system. For the system in Fig. 1, a drawback of a low coupling coefficient between the Tx and Rx coils, as they locate a distance away from each other, is possibly overcome by using high-Q coils. This may help improve the system performance. In other words, the system is able to maintain the high efficiency even when the receiver moves far away from the transmitter. In the transmitting part, a signal generator is used to generate a sinusoidal signal oscillating at the frequency of interest. A power of the output signal from the generator is too small,

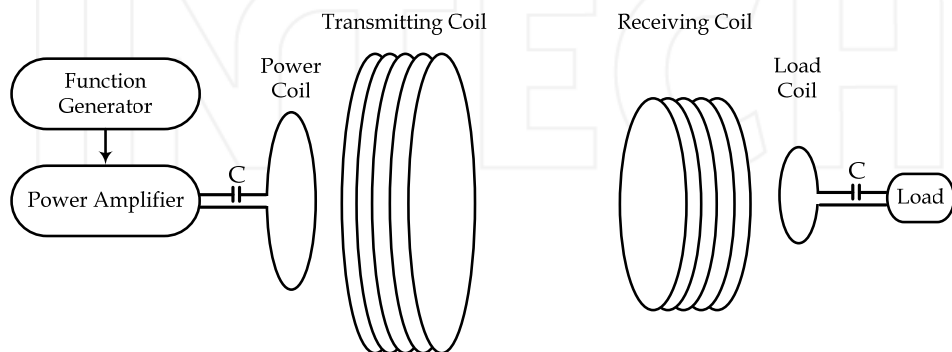


Fig. 1. Model of wireless power transfer system.

approximately tens to hundreds of milliwatts, to power devices of tens of watts. Hence, this signal is delivered to the Tx coil through a power amplifier for signal power amplification. In the receiver side, the receiving resonator and then load coil will transfer the induced energy to a connected load such as a certain electronic device. While the efficiency of the two-coil counterpart is unproportionally dependent on an operating distance, the four-coil system is less sensitive to changes in the distance between the Tx and Rx coils. This kind of system can be optimized to provide a maximum efficiency at the given operating distance. These characteristics will be analyzed in the succeeding sections.

## 2.1 Circuit analysis of four-coil system

Fig. 2 shows the circuit representation of the four-coil system as modeled above. The schematic is composed of four resonant circuits corresponding to the four coils. These coils are connected together via a magnetic field, characterized by coupling coefficients  $k_{12}$ ,  $k_{23}$ , and  $k_{34}$ . Because the strengths of cross couplings between the power & Rx coils and the load & Tx coils are very weak, they can be neglected in the following analysis. Theoretically, the coupling coefficient (also called coupling factor) has a range from 0 to 1. If all magnetic flux generated from a transmitting coil is able to reach a receiving coil, the coupling coefficient would be "1". On the contrary, the coefficient would be represented as "0" when there is no interaction between them. Actually, there are some factors identifying the coupling coefficient. It is effectively determined by the distance between the coils and their relative sizes. It is additionally determined by shapes of the coils and orientation (angle) between them. The coupling coefficient can be calculated by using a given formula

$$k_{xy} = \frac{M_{xy}}{\sqrt{L_x L_y}} \quad (1)$$

where  $M_{xy}$  is mutual inductance between coil "x" and coil "y" and note that  $0 \leq k_{xy} \leq 1$ . Referring to the circuit schematic, an AC power source with output impedance of  $R_s$  provides energy for the system via the power coil. Normally, the AC power supply can be either a power amplifier or a vector network analyzer (VNA) which is useful to measure a transmission and reflection ratio of the system. Hence, a typical value of  $R_s$ , known as the output impedance of the power amplifier or the VNA, is  $50 \Omega$ . The power coil can be modeled as an inductor  $L_1$  with a parasitic resistor  $R_1$ . A capacitor  $C_1$  is added to make the power coil resonate at the desirable frequency. The Tx coil is a helical coil with many turns represented as an inductor  $L_2$  with parasitic resistance  $R_2$ . Geometry of the Tx coil

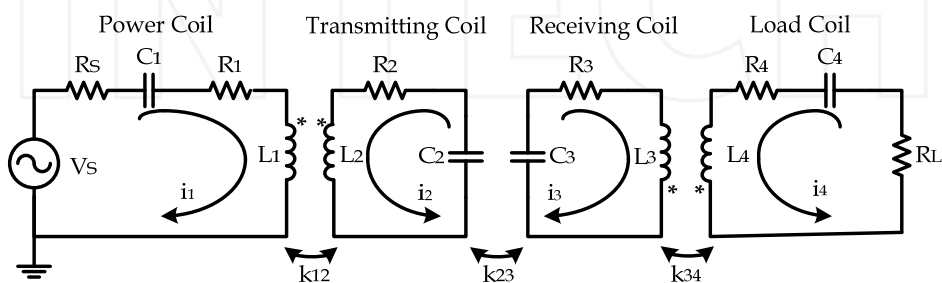


Fig. 2. Equivalent circuit of four-coil system.

determines its parasitic capacitance such as stray capacitance, which is represented as  $C_2$ . Since this kind of capacitance is difficult to be accurately predicted, for fixed size of the coil, a physical length, which impacts the self-inductance and the parasitic capacitance, has been manually adjusted in order to fit the resonant frequency as desired. In the receiver side, the Rx coil is modeled respectively by  $L_3$ ,  $R_3$  and  $C_3$ . The load coil and the connected load are also performed by  $L_4$ ,  $R_4$  and  $R_L$ . A capacitor  $C_4$  also has the same role as  $C_1$ , so that the resonant frequency of the load coil is defined. When the frequency of sinusoidal voltage source  $V_S$  is equal to the self-resonant frequency of the resonators, their impedances are at least. In the other words, currents of the coils would be at the most and energy can be delivered mostly to the receiving coil. Otherwise, energy of the transmitting power source would be dissipated in the power coil circuit itself, resulting in the very low efficiency. In general, setting the frequency of AC supply source as same as the natural resonant frequency of the transceiver coils is one of key points to achieve a higher performance of the system.

As can be seen from Fig. 2, the Tx coil is magnetically coupled to the power coil by the coupling coefficient  $k_{12}$ . In fact, the power coil is one of the forms of impedance matching mechanism. The same situation experiences in the receiving part where the Rx coil and load coil are magnetically linked by  $k_{34}$ . The strength of interaction between the transmitting and receiving coils is characterized by the coupling coefficient  $k_{23}$ , which is decided by the distance between these coils, a relative orientation and alignment of them. In general, it is able to use other mechanisms for the impedance matching purpose in either or both sides of the system. For example, a transformer or an impedance matching network, which consists of a set of inductors and capacitors configured to connect the power source and the load to the resonators, is routinely employed. Similar to aspects mentioned above, in reality, the power and Tx coils would be implemented monolithically for the sake of convenience; hence the coupling coefficient  $k_{12}$  would be stable. For the same objective,  $k_{34}$  would also be fixed. Therefore, there only remains coefficient  $k_{23}$  which is so-called an environment variable parameter. The parameter varying with usage conditions, may include the range between the resonator coils, a relative orientation and alignment between them and a variable load on the receiving resonator.

The circuit model offers a convenient way to systematically analyze the characteristic of the system. By applying circuit theory Kirchhoff's Voltage Law (KVL) to this system, with the currents in each resonant circuit chosen as illustrated in Fig. 2, a relationship between currents through each coil and the voltage applied to the power coil can be captured as a following matrix

$$\begin{bmatrix} V_S \\ 0 \\ 0 \\ 0 \end{bmatrix} = \begin{bmatrix} Z_1 & j\omega M_{12} & 0 & 0 \\ j\omega M_{12} & Z_2 & -j\omega M_{23} & 0 \\ 0 & -j\omega M_{23} & Z_3 & j\omega M_{34} \\ 0 & 0 & j\omega M_{34} & Z_4 \end{bmatrix} \begin{bmatrix} i_1 \\ i_2 \\ i_3 \\ i_4 \end{bmatrix} \quad (2)$$

where  $Z_1$ ,  $Z_2$ ,  $Z_3$ , and  $Z_4$  respectively are loop impedances of the four coils. These impedances can be indicated as below

$$Z_1 = R_S + R_1 + j\left(\omega L_1 - \frac{1}{\omega C_1}\right) \quad (3)$$

$$Z_2 = R_2 + j \left( \omega L_2 - \frac{1}{\omega C_2} \right) \quad (4)$$

$$Z_3 = R_3 + j \left( \omega L_3 - \frac{1}{\omega C_3} \right) \quad (5)$$

$$Z_4 = R_L + R_4 + j \left( \omega L_4 - \frac{1}{\omega C_4} \right) \quad (6)$$

From the matrix (2), by using the substitution method, the current in the load coil resonant circuit is derived as given

$$i_4 = - \frac{j\omega^3 M_{12} M_{23} M_{34} V_s}{Z_1 Z_2 Z_3 Z_4 + \omega^2 M_{12}^2 Z_3 Z_4 + \omega^2 M_{23}^2 Z_1 Z_4 + \omega^2 M_{34}^2 Z_1 Z_2 + \omega^4 M_{12}^2 M_{34}^2} \quad (7)$$

It is clearly seen that the voltage across the load is equal to  $V_L = -i_4 R_L$  and the relationship between the voltages of source and load is given as  $V_L/V_s$ .

The system model can be considered as a two port network. To analyze a figure of merit of this kind of system, S - parameter is a suitable candidate. Actually,  $S_{21}$  is a vector referring to a ratio of signal exiting at an output port to a signal incident at an input port. This parameter is really important because a power gain, the critical factor determining of power transfer efficiency, is given by  $|S_{21}|^2$ , the squared magnitude of  $S_{21}$ . The parameter of  $S_{21}$  is calculated by (Sample et al., 2011, as cited in Fletcher & Rossing, 1998; Mongia, 2007)

$$S_{21} = 2 \frac{V_L}{V_s} \left( \frac{R_s}{R_L} \right)^{1/2} \quad (8)$$

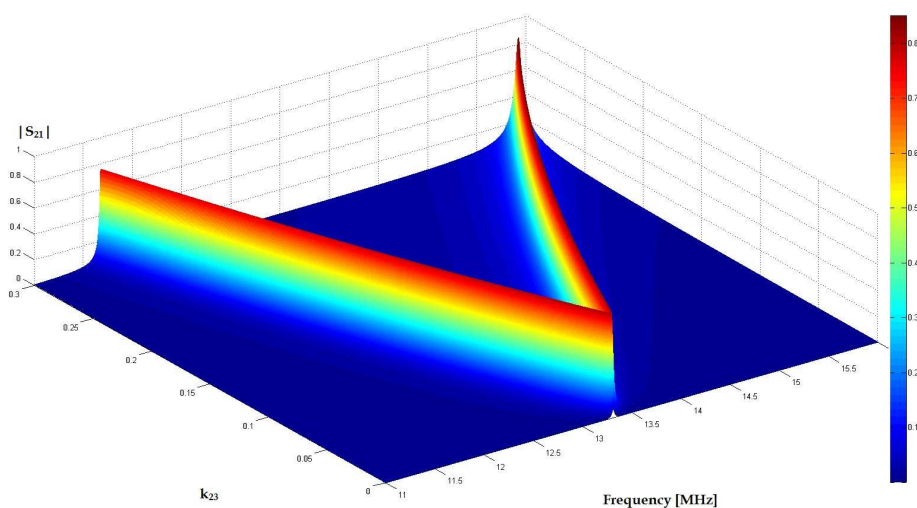
Thus, combining with  $M_{xy} = k_{xy} \sqrt{L_x L_y}$  derived from (1), the  $S_{21}$  parameter is given as

$$S_{21} = \frac{j2\omega^3 k_{12} k_{23} k_{34} L_2 L_3 \sqrt{L_1 L_4 R_s R_L}}{Z_1 Z_2 Z_3 Z_4 + k_{12}^2 L_1 L_2 Z_3 Z_4 \omega^2 + k_{23}^2 L_2 L_3 Z_1 Z_4 \omega^2 + k_{34}^2 L_3 L_4 Z_1 Z_2 \omega^2 + k_{12}^2 k_{34}^2 L_1 L_2 L_3 L_4 \omega^4} \quad (9)$$

It is helpful to analyze the performance of the system according to equation (9). With all the circuit parameters provided in Table 1, the parameter regarded as the factor determining the efficiency of the system, magnitude of  $S_{21}$ , can be performed by a function of only two variables  $k_{23}$  and frequency. As referred, the coupling coefficient  $k_{23}$  is the parameter which varies according to changes in circumstances. A changeable distance, for instance, is a cause of  $k_{23}$  variation. In addition, changes in the orientation or misalignment between the transmitting and receiving resonators make the above coefficient inconsistent as well. Actually, when the distance increases,  $k_{23}$  will go down because the mutual inductance between those coils declines with distance. In case of a variable orientation or misalignment, the  $k_{23}$  also changes. The relation among  $|S_{21}|$ ,  $k_{23}$  and frequency is demonstrated in Fig. 3. Note that in practice, a vector of  $S_{21}$  parameter including magnitude and phase information can be measured by using VNA. From Fig. 3, it is clearly seen that when  $k_{23}$  is small in cases of the large distance between the transmitter and the receiver or the misalignment, orientation deviation taking place, the efficiency represented as  $S_{21}$  magnitude is able to

Transmitter Side		Receiver Side	
Parameter	Value	Parameter	Value
$R_S$	50 $\Omega$	$L_3$	0.4 $\mu\text{H}$
$L_1$	0.5 $\mu\text{H}$	$R_3$	0.02 $\Omega$
$R_1$	0.015 $\Omega$	$C_3$	357.5 pF
$C_1$	286 pF	$k_{34}$	0.1
$k_{12}$	0.05	$L_4$	0.1 $\mu\text{H}$
$L_2$	1.3 $\mu\text{H}$	$R_4$	0.012 $\Omega$
$R_2$	0.03 $\Omega$	$C_4$	1.43 nF
$C_2$	110 pF	$R_L$	50 $\Omega$
$k_{23}$	0.0001 to 0.3	frequency	11-16 MHz

Table 1. An example of circuit values.

Fig. 3.  $|S_{21}|$  as a function of  $k_{23}$  and frequency (3D – View).

reach a peak at the self resonant frequency of approximately 13.3 MHz. However, the resonant frequency separates as  $k_{23}$  is over a certain level. The phenomenon is so-called frequency splitting which has a negative impact on the system efficiency. For instance, as long as the transmitting and receiving coils are such closed as the coupling coefficient  $k_{23}$  between them is 0.1, the resonant frequency splits into two peaks at 12.69 and 14.03 MHz as observed from Fig. 3. Consequently, the system performance is considerably degraded. In order to overcome the drawback, an automatically frequency tuning circuit is proposed, as presented in Section 3. The circuit is used to track the resonant frequency of interest so as to preserve the efficiency of the system in cases of transceivers' mobility. It is possible to simulate the system by using Advanced Design System (ADS) of Agilent Technologies. With the circuit setup illustrated in Fig. 4, the result of the magnitude of  $S_{21}$  can be obtained as shown in Fig. 5.

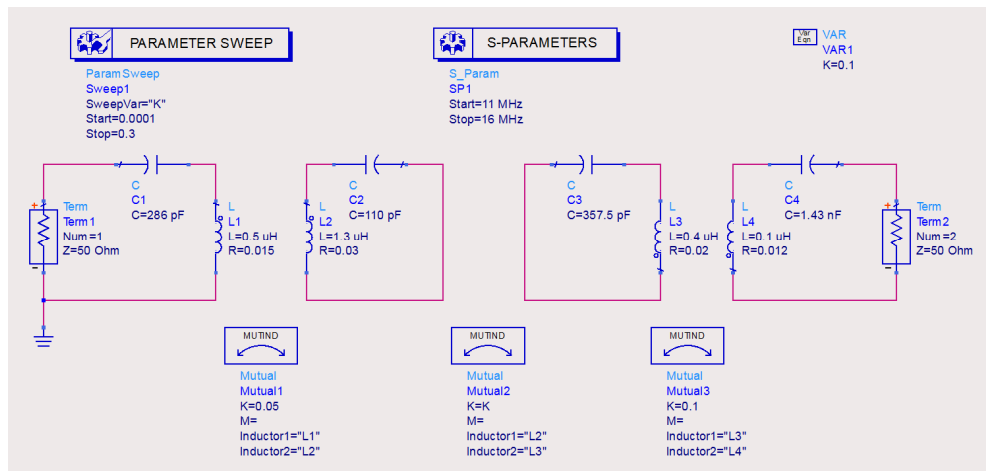


Fig. 4. Simulation setup using Advanced Design System (ADS).

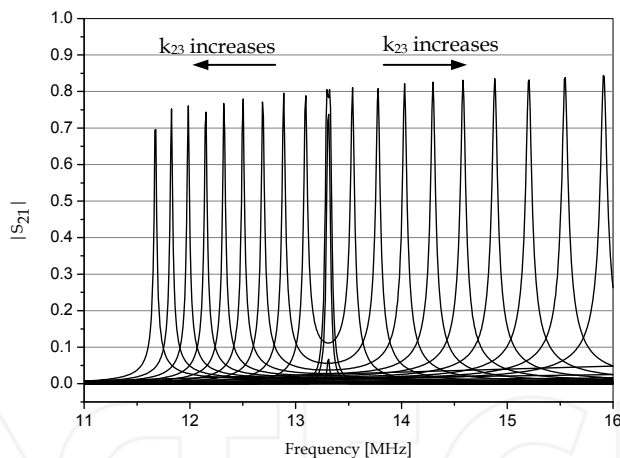


Fig. 5. Simulation result showing  $|S_{21}|$  as a function of  $k_{23}$  and frequency (2D - View).

It is instructive to analyze carefully a trend of  $|S_{21}|$  as  $k_{23}$  variation. Fig. 5 clarifies that when the coefficient  $k_{23}$  is absolutely small corresponding to a case that the transmitter and the receiver are too far away each other,  $|S_{21}|$  is low. When the distance between the resonators is getting closer,  $k_{23}$  increases bringing about a higher magnitude of  $S_{21}$ . However, as  $|S_{21}|$  increases to a certain level, the higher  $k_{23}$  does not lead to the higher amount of  $|S_{21}|$ . Moreover, there is the frequency splitting issue which substantially reduces the system efficiency. The point, at which the deviation of the original resonant frequency (13.3 MHz) happens, plays a prominent role in the system. It clarifies the relative position of the resonators that the performance of the system is the highest. If the distance is longer than that range, the efficiency is poorly defined. On the contrary, the resonant frequency detunes

along two furrows, but the efficiency is still high. Thus, it would be the maximum power transfer if the frequency can be tuned to the desirable frequency.

Coming back the system equation indicated in (9), let expand this equation in terms of quality factor which appreciates how well the resonator can oscillate. The quality factor is presented in a formula as given below

$$Q_i = \frac{1}{R_i} \sqrt{\frac{L_i}{C_i}} = \frac{\omega_i L_i}{R_i} \Leftrightarrow \omega_i L_i = R_i Q_i, i = 1 \sim 4 \quad (10)$$

where  $\omega_i$  and  $R_i$  are respectively the self-resonant frequency and equivalent resistance of each resonant circuit. In the power coil, for instance,  $R_i$  is a sum of  $R_S$  and  $R_1$ . Actually,  $\omega_i$  of each coil is defined to be the same,  $\omega_1 = \omega_2 = \omega_3 = \omega_4 = \omega_0$ . When the resonance takes place, the total impedance of each coil is presented as following

$$Z_1 = R_S + R_1 \approx R_S \quad (11)$$

$$Z_2 = R_2 \quad (12)$$

$$Z_3 = R_3 \quad (13)$$

$$Z_4 = R_L + R_4 \approx R_L \quad (14)$$

For simplicity, in addition to the fact that system parameters can be measured by VNA, it is common to set  $R_S$  equal to  $R_L$ . At the resonant frequency,  $\omega_0 = 1 / \sqrt{L_i C_i}$ , from (9), the magnitude of  $S_{21}$  can be written as

$$|S_{21}| = \frac{2k_{12}k_{23}k_{34}Q_2Q_3\sqrt{Q_1Q_4}}{1 + k_{12}^2Q_1Q_2 + k_{23}^2Q_2Q_3 + k_{34}^2Q_3Q_4 + k_{12}^2k_{34}^2Q_1Q_2Q_3Q_4} \quad (15)$$

As referred previously, the coupling coefficient  $k_{12}$  and  $k_{34}$  would be constant. There is only  $k_{23}$  varying with medium conditions. To find the range between the resonators at which  $|S_{21}|$  or the efficiency is certainly at maximum, a derivative of  $S_{21}$  with respect to  $k_{23}$  is taken and then setting the result to zero, yielding

$$\frac{d|S_{21}|}{dk_{23}} = 0 \Rightarrow k_{23}^* = \sqrt{\frac{(1 + k_{12}^2Q_1Q_2)(1 + k_{34}^2Q_3Q_4)}{Q_2Q_3}} \quad (16)$$

This value of  $k_{23}^*$  is equivalent to the maximum range that the transmitter is able to effectively transfer power to the receiver at the given resonant frequency (before the resonant frequency breaking in two peaks). Note that  $k_{23}^* \leq 1$ . With the purpose of finding out the maximum efficiency of the system in terms of  $|S_{21}|$ , it is feasible to substitute  $k_{23}$ , which is derived above, into equation (15)

$$|S_{21}|_{\max} = \frac{k_{12}k_{34}Q_1Q_4R_L}{k_{23}^*\sqrt{L_1\omega_1L_4\omega_4}} = \frac{k_{12}k_{34}Q_1Q_4R_L}{k_{23}^*\sqrt{L_1L_4}\omega_0} \quad (17)$$



It is clear that  $|S_{21}|_{\max}$  unproportionally depends on  $k_{23}^*$ . It means for the sake of a higher efficiency, the extent that the highest efficiency can be achievable is shortened. In order to get a greater value of  $|S_{21}|_{\max}$ ,  $k_{23}^*$  is supposed to decrease. From equation (16), increasing  $Q_2$  and  $Q_3$  is able to reduce the  $k_{23}^*$ . In general, making the very high-Q transmitting and receiving coils is very crucial so as to achieve the high transfer performance.

For example, from equation (17), with the value given in Table 1, the maximum value of magnitude of  $S_{21}$  parameter is calculated as follows

$$\begin{aligned}\omega_0 = \omega_1 &= \frac{1}{\sqrt{L_1 C_1}} \approx 83.624 \times 10^6 \text{ [rad / s]} \\ Q_1 &= \frac{\omega_0 L_1}{R_S + R_1} \approx 0.84 \\ Q_2 &= \frac{\omega_0 L_2}{R_2} \approx 3623.71 \\ Q_3 &= \frac{\omega_0 L_3}{R_3} \approx 1672.48 \\ Q_4 &= \frac{\omega_0 L_4}{R_L + R_4} \approx 0.17 \\ k_{23}^* &= \sqrt{\frac{(1 + k_{12}^2 Q_1 Q_2)(1 + k_{34}^2 Q_3 Q_4)}{Q_2 Q_3}} \approx 2.34 \times 10^{-3} \\ |S_{21}|_{\max} &= \frac{k_{12} k_{34} Q_1 Q_4 R_L}{k_{23}^* \sqrt{L_1 L_4} \omega_0} \approx 0.82\end{aligned}$$

## 2.2 Different coupling mechanism systems in wireless power transfer

As mentioned in Subsection 2.1, the advantage of the four coils system over the two coils system is a high efficiency even in far afield condition. Why is that so? To answer this question, it is instructive to study three different coupling mechanism based circuits which are demonstrated in Fig. 6. A non-resonant inductive coupling circuit in Fig. 6(a) is totally based on the principle of an ordinary transformer. This kind of power transfer also uses primary and secondary coils as similar as transformer, but a striking feature is an exclusion of a high permeability coil. Since an energy transmission is relied on the induction principle, more power is dissipated along the coil or ambient environment and it is more difficult to achieve a long distance transmission.

The above limitation can be overcome using the WPT based on resonant coupling shown in Fig. 6(b). By adding external capacitors, coils in primary and secondary side are able to resonate at the same frequency of interest. In fact, high quality factor coils are considered as one of the most critical features for a superior system.

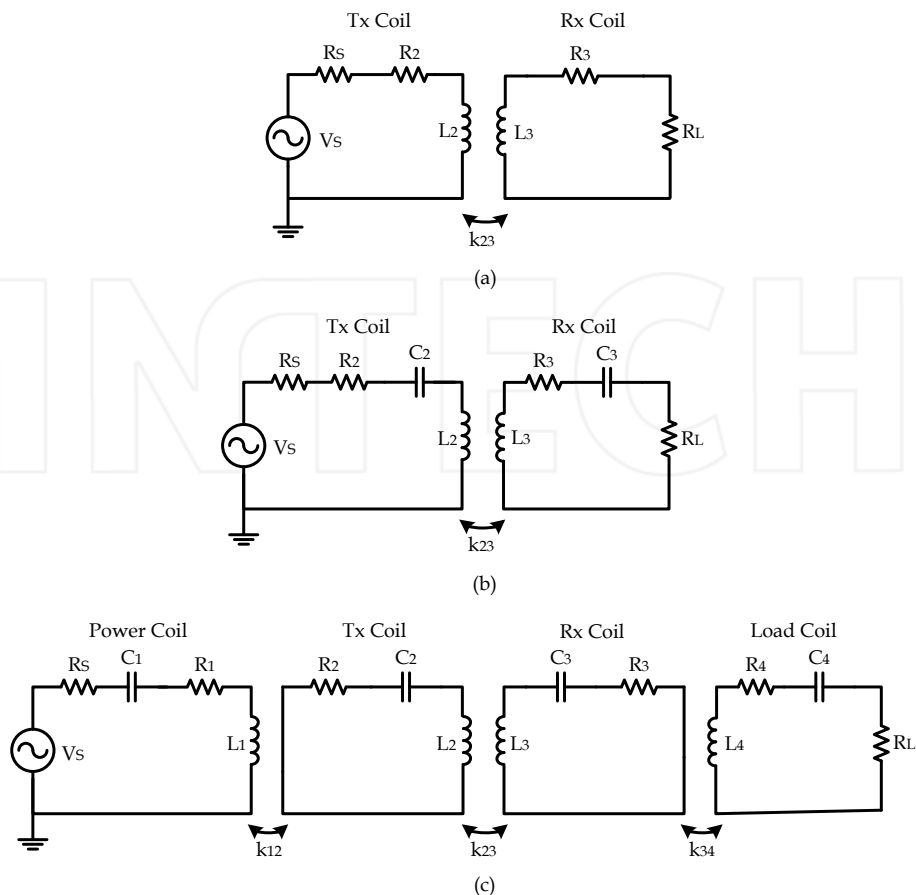


Fig. 6. Three different coupling mechanism circuits.

- Non-resonant inductive coupling based circuit.
- Low-Q resonant coupling based circuit (two-coil system).
- High-Q resonant coupling based circuit (four-coil system).

In case of Fig. 6(b), quality factors of the two resonant circuits are determined by the loading provided by  $R_S$  and  $R_L$  which are also two major contributors to loss of circuits (Cannon et al., 2009). Source and load resistances are leading causes of lower Q resonators, deteriorating the system efficiency. A solution for this matter is to separate the  $R_S$  and  $R_L$  from the resonators, that is illustrated in Fig. 6(c). Certainly, the resonators have larger quality factors due to the elimination of the unexpected resistances. It is apparent that the quality factors of the transmitting and receiving coils dominantly affect the system performance. In order to comprehend more deeply about the three different circuits, an example with circuit parameters shown in Table 2 is put forward. Fig. 7 illustrates a comparison result of the three different coupling methods including inductive coupling, low-Q resonant coupling and high-Q resonant coupling. Note that the two resonant coupling circuits resonate at 8 MHz.

Transmitter Side		Receiver Side	
Parameter	Value	Parameter	Value
$R_5$	$50\ \Omega$	$L_3$	$5\ \mu\text{H}$
$L_1$	$2\ \mu\text{H}$	$R_3$	$0.7\ \Omega$
$R_1$	$0.4\ \Omega$	$C_3$	$79.2\ \text{pF}$
$C_1$	$198\ \text{pF}$	$k_{34}$	$0.1$
$k_{12}$	$0.1$	$L_4$	$1\ \mu\text{H}$
$L_2$	$30\ \mu\text{H}$	$R_4$	$0.25\ \Omega$
$R_2$	$2\ \Omega$	$C_4$	$396\ \text{pF}$
$C_2$	$13.2\ \text{pF}$	$R_L$	$50\ \Omega$
$k_{23}$	$0.001$	frequency	$4 - 12\ \text{MHz}$

Table 2. Example of component values for three circuit models.

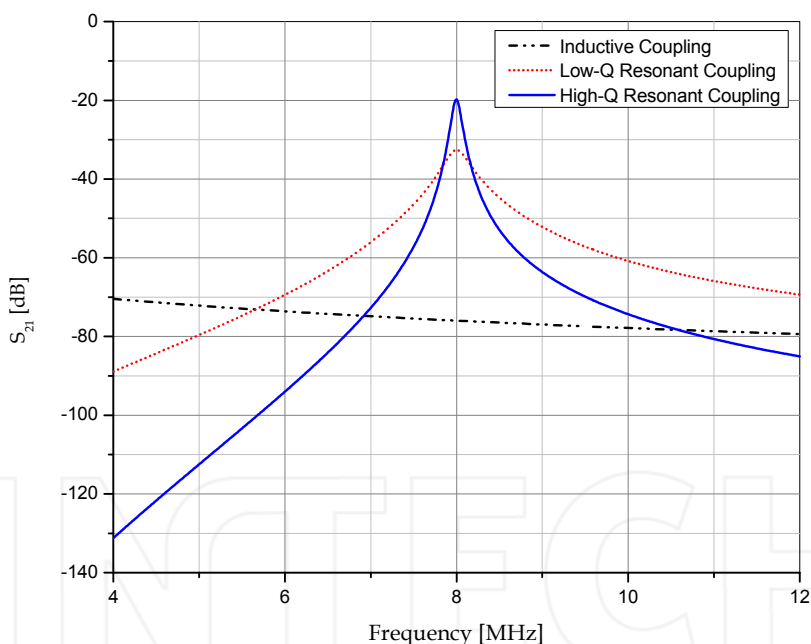


Fig. 7. Comparison result of three different types of coupling.

As can be seen, the value of  $S_{21}$  in dB is used for the comparison. It is evident that for the inductive coupling mechanism shown in Fig. 6(a), the parameter of  $S_{21}$  is the lowest. In fact, this value gradually declines from -70 dB to about -80 dB for a frequency range between 4 and 12 MHz. By above analysis, the Q factor of the circuit shown in Fig. 6(c) is much greater than that of Fig. 6(b). In fact, from Fig. 7,  $S_{21}$  parameter of the high-Q circuit is approximately 20 dB higher than that of the low-Q circuit. That completely proves the theoretical presumption.

### 2.3 Wireless energy transmission to multiple devices through resonant coupling

All the approaches mentioned previously are merely in terms of one to one WPT. That means one transmitter, which includes a power coil and a transmitting coil, provides energy wirelessly to only one receiver consisting of receiving and load coils in a distance away. In reality, however, the cases of multiple small receivers are in favor and needed to be considered carefully. Transferring power to a couple of receivers is also based on the same principle as one to one case. Nevertheless, an effect of two receivers in proximity is considerable. Thus, several cases of multiple receivers wireless energy transmission will be investigated. In case of two identical receivers located sufficiently far field and there is no interaction between them, the system can be interpreted as a sum of two discrete systems. Since the two receivers are identical, their operations are coincident with each other if they experience a same condition such as the strength of coupling. With the circuit parameters shown in Table 2, only difference in the coupling coefficient between the transmitting and receiving coils, the performance of the two receivers is illustrated in Fig. 8. It is undoubtedly true that the resonant frequency splits into two peaks as an increase of  $k$ , which is the coupling coefficient between the two receivers and the transmitter. The stronger the coupling is, the more the new resonant frequencies deviate from the original resonant frequency. At  $k$  of 0.01, for example, the system efficiency hits the peak at 8 MHz. When the coupling getting stronger to 0.145 and then 0.3, the original peak respectively breaks in two other peaks at about 7.2 and 9.1 MHz; 6.7 and 10.6 MHz. On the other hand, as shown in Fig. 9, in case of the strong interaction between receiving coils, even at low  $k$ , the resonant frequency is splitted to two peaks at 7 and 8 MHz. When  $k$  reaches 0.145, the maximum power transfer occurs at the frequency of 6.7 and 8.5 MHz. The separation among splitted frequencies is larger at the stronger coupling between the transmitter and the receivers, 6.3 and 9.6 MHz. For a situation that the two receivers resonate at the same frequency but their

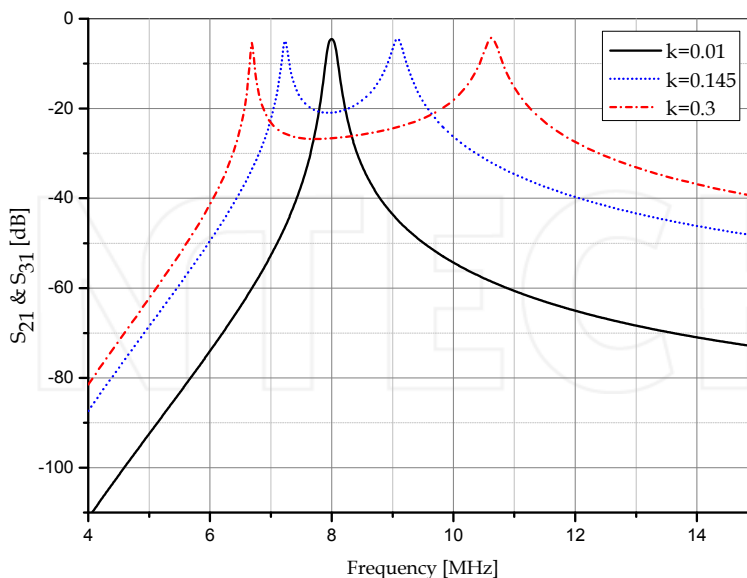


Fig. 8. Performance of two identical receivers in case of no interaction between them.

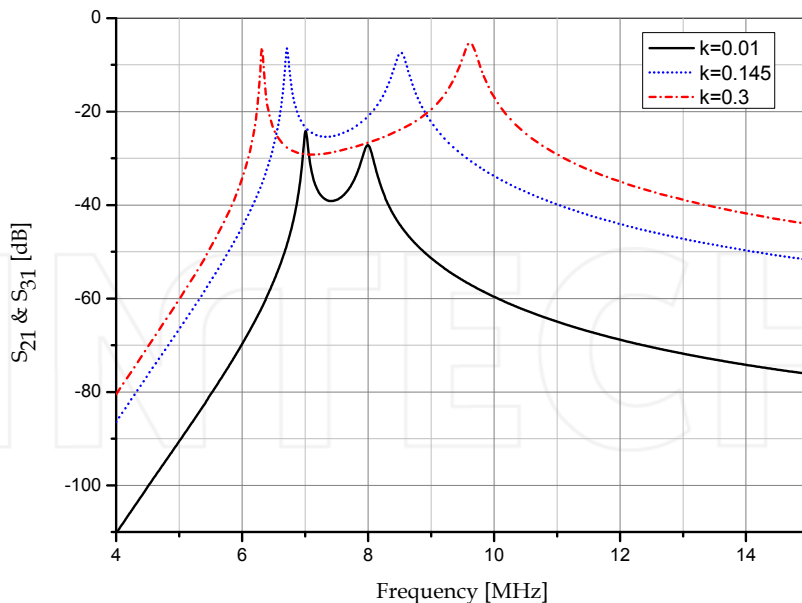


Fig. 9. Performance of two identical receivers in case of strong interaction.

physical parameters are different, the system transfer efficiency is relatively similar. Theoretically, the four circuit model equations derived from the matrix equation (2) can be extended for multiple receivers. For one to two system, in particular, the extension of circuit equations is straightforward, with six equations instead of four. By using these equations, it is possible to predict the characteristic of the system with multiple receivers.

## 2.4 Experimental results

An experiment, which is conducted for WPT, was presented (Imura & Hori, 2011). The experimental setup is illustrated in Fig. 10. For S - parameter measurement, a transmitter and a receiver of the power transmission system are in turn connected to port 1 and port 2 of VNA. As same as theoretical analysis, the transmitting and receiving antennas resonate at same frequency. The helical antennas used are short- type antennas, which have separate excitation using self-inductances and added capacitors. These antennas have only one turn each with a radius of 150 mm and attached capacitors in series to adjust the resonant frequency of interest. The experiment is conducted with the distance between two antennas respectively 49, 80, 170 and 357 mm. From Fig. 11, at the closed distance of 49 mm, the system achieves the highest efficiency, represented as the squared magnitude of  $S_{21}$  parameter, at the two peaks of roughly 12.4 and 15.2 MHz. When the distance is getting smaller, the resonant frequency separation reduces, about 12.7 and 14.6 respectively. And at the distance of 170 mm, the two splitted frequencies converge at approximately 13.6 MHz. The efficiency significantly degrades with the increasing distance. The special point distinct from the presented model of WPT is that there are no power coil and load coil in this model. The authors used two resonators in addition to impedance matching structures instead of

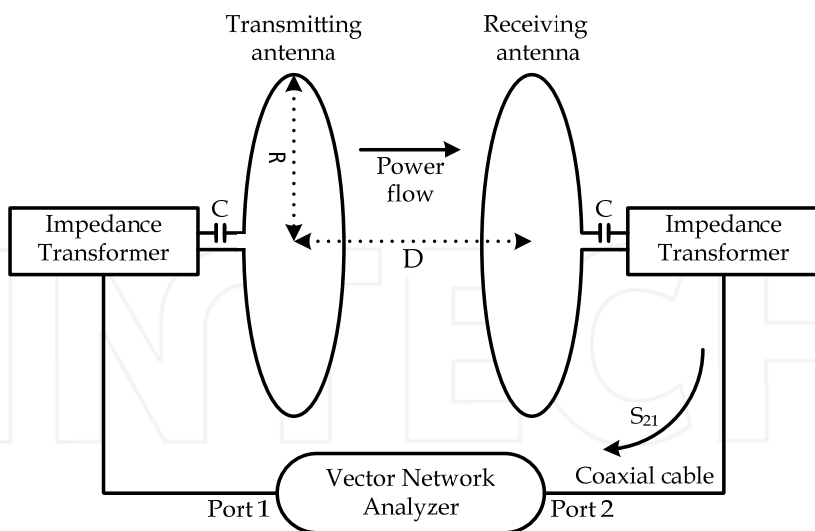
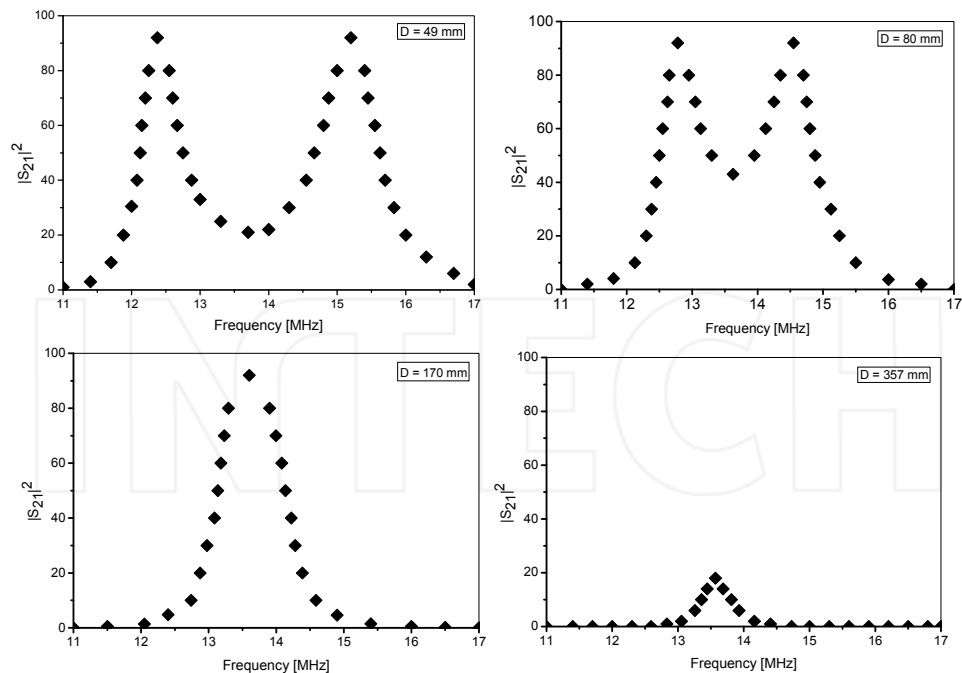


Fig. 10. Experiment setup.

Fig. 11. Efficiency, represented as  $|S_{21}|^2$ , versus frequency at different distances.

the four-coil system. The advantage of this model is a possibility of eliminating the magnetically coupled coils so that the system would be simplified. Nonetheless, the benefits of cross-coupling effect increasing the system efficiency in the low-mode of resonant frequencies can be cancelled out (Sample et al., 2011).

### 3. Maximizing efficiency with adaptive circuits

From the above analysis of the relationship between the system efficiency and the resonant frequency, it is clear that the operating frequency is the critical factor determining the performance of the system. Besides, the flexibility of impedance matching structures also plays an important role enabling high transfer efficiency (Chen et al., 2010). Of considerable interest for applications of WPT relied on electromagnetic resonance, the cases of mobile receiver or multiple receivers are absolutely typical. However, there exists a drawback that degenerates the efficiency in these cases. In fact, the transfer efficiency significantly decreases with distance variations between the transmitter and the receiver or in case of multiple receivers. In order to overcome the limitations, adaptive circuits are proposed. These circuits are so-called ALL which help to maintain the optimal resonant condition and realize the maximum wireless power transfer efficiency as well.

#### 3.1 Efficiency optimization based on frequency control

For the situation of one transmitter and one portable receiver, the transfer efficiency represented as  $|S_{21}|$ , which the function of the distance, the relative orientation and alignment between the resonators, is analytically clarified in the previous section. Remind that magnitude of  $S_{21}$  parameter is relatively small when a transmitter and a receiver are too far away. When they get approach each other,  $|S_{21}|$  goes up and at a certain point, the phenomenon of frequency splitting occurs degrading the system performance. Therefore, an optimal control mechanism of efficiency based on frequency control is needed to stabilize the transfer efficiency.

Generally, a range of control frequency is confined, with a high limit caused by the coil characteristic and a low limit due to the low efficiency. In that range, the frequency can be determined and tuned in order for high efficiency to be achieved. From the equations (7) and (8), it is possible to derive a following equation

$$S_{21} = \frac{j2\omega^3 M_{12} M_{23} M_{34} R_L}{Z_1 Z_2 Z_3 Z_4 + \omega^2 M_{12}^2 Z_3 Z_4 + \omega^2 M_{23}^2 Z_1 Z_4 + \omega^2 M_{34}^2 Z_1 Z_2 + \omega^4 M_{12}^2 M_{34}^2} \quad (18)$$

In which mutual inductance  $M_{23}$  is calculated by using Neumann formula (Imura & Hori, 2011, as cited in Sallan et al., 2009)

$$M_{23} = \frac{\mu_0}{4\pi} \int_{C_2} \int_{C_3} \frac{dl_2 dl_3}{D} \quad (19)$$

However, due to complicated calculations, it is reasonable to use an approximation of the mutual inductance given as below (Karalis et al., 2008 as cited in Jackson, 1999)

$$M_{23} \approx \pi \mu_0 (r_2 r_3)^2 \frac{N_2 N_3}{2D^3} \quad (20)$$

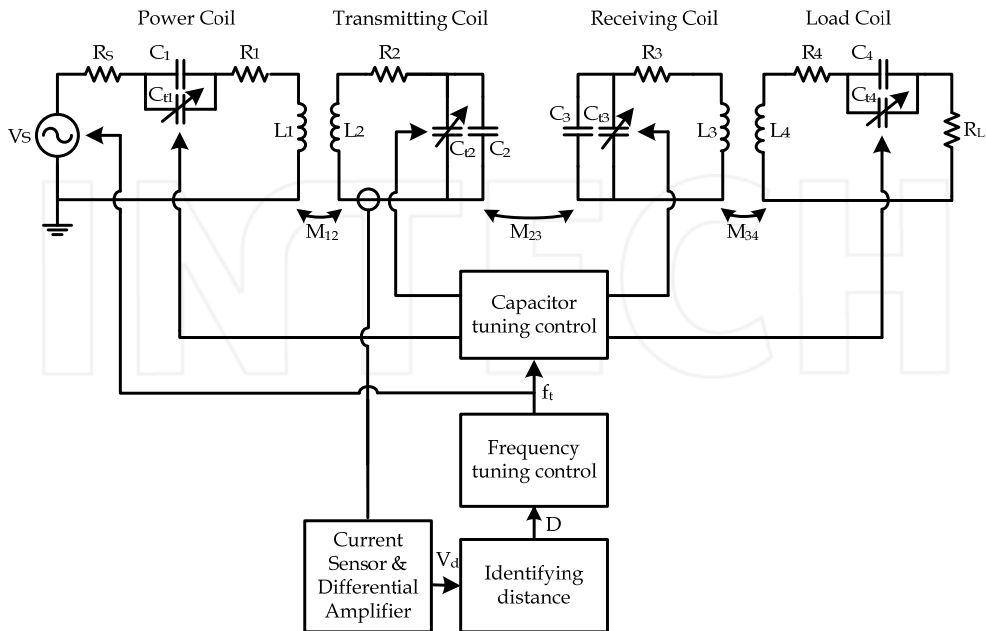


Fig. 12. Adaptive circuit of frequency control.

Note that in (18), typically, almost all components would be identified with given specifications of circuit setup including radius of coils' cross-section  $a$ , number of turns  $N$ , radius of coils  $r_i$  ( $i=2,3$ ), and distance between power coil, load coil and resonators. So, by substituting (19) into (18), there are merely the three unknown variables of frequency  $\omega$ ,  $S_{21}$  parameter and distance between the resonators  $D$ . With the given requirement of efficiency, represented as the magnitude of  $S_{21}$ , and identified distance between the resonators, it is able to figure out the frequency of interest. An adaptive circuit used to stabilize the system transfer efficiency is demonstrated in Fig. 12. A current sensor is used to detect a current flow in the transmitting coil. Due to the fact that the transmitting coil is not connected to the ground, the sensed signal is in terms of differential signal. The signal is then compared with reference sources in an adjacent block, hence it is essential to utilize a differential amplifier in order to transform the differential signal to a single-ended signal. An output voltage of  $V_d$  is then switched to a block of distance identification, where  $V_d$  is in turn compared with reference voltages to determine a distance between the resonators. Like the preceding analysis, with the found parameter, a new tuned  $f_t$  is established. This frequency is the wanted frequency of the power source as well. Subsequently, in order to control all coils resonating at the frequency of  $f_t$ , a capacitor tuning control block is required to control variable capacitors attached at each coil as below



$$f_t = \frac{1}{2\pi L_i C_{total-i}}, i = 1 \sim 4 \quad (21)$$

$$C_{ti} = C_{total-i} - C_i, i = 1 \sim 4 \quad (22)$$

Note that  $C_2$  and  $C_3$  here are lumped components representing approximately the parasitic capacitances of the transmitting and receiving coils. The capacitors  $C_{ti}$  with  $i$  from 1 to 4 are respectively connected in parallel with the capacitors of four coils.

In general, when the frequency tuning mechanism is enabled, the controller picks the resonant frequency of interest and tracks it as the receiver is moved away from the transmitter.

### 3.2 Efficiency optimization based on impedance matching control

In addition to the efficiency optimization technique based on frequency tuning, impedance matching tuning method is a potential candidate for an adaptive circuit that also maximizes the system efficiency. In some cases, the usage of wide range of frequency tuning has limitations that can affect these other bands such as ISM bands which were internationally reserved. Thus, utilizing the technique of flexible impedance matching is really essential.

In fact, by changing the strength of coupling between the load coil and the resonator and slightly retuning the receiving coil, it is possible to achieve the maximum transfer efficiency (Chen et al., 2010, as cited in Kurs et al., 2007). For practical interest, however, an adjustment in the coupling coefficient between the coils in the transmitting part is preferred. The change in coupling strength can be made by varying the distance between those coils, the relative orientation and alignment of them. However, it is not viable to automatically control them in the system consisting of four coils. Thus, a model of two resonators and other impedance matching structure is used. A circuit of adaptive impedance matching in the transmitter side is shown in Fig. 13. Based on a current sensed from the transmitting resonator, a control circuit block is able to identify distance variations, different orientation, misalignment between the resonators or in case of multiple receivers, then automatically control a power amplifier (PA) and a tunable impedance matching block so as to maximize the transfer efficiency. Actually, for situations of relatively large distance length, significantly different orientation or misalignment between the two resonators, in spite of utilizing the adaptive impedance matching, increasing the output power of the power amplifier is recommended to improve the system transfer efficiency. The striking feature of the circuit is that the system frequency is fixed and it is very helpful in many applications.

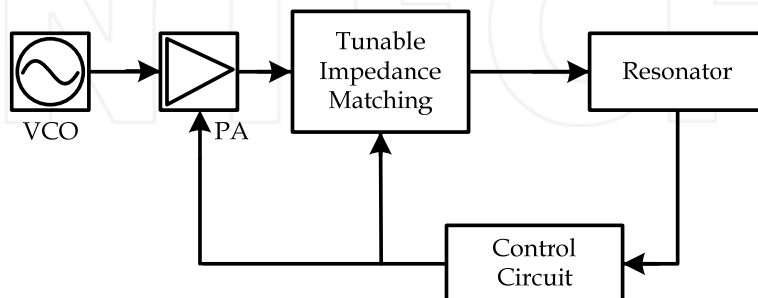


Fig. 13. Adaptive circuit of impedance matching control in transmitter side

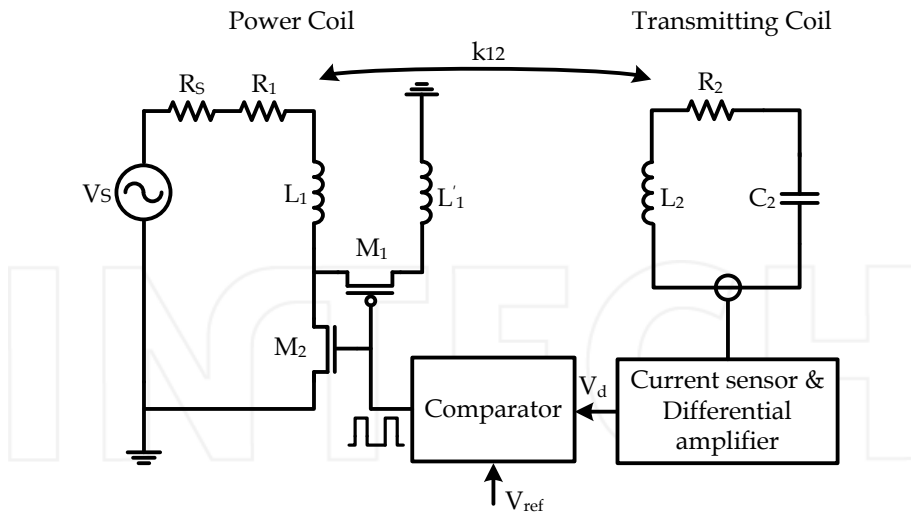


Fig. 14. Adaptive circuit of Q-tuning.

### 3.3 Adaptive Q tuning circuit

From the analysis of different coupling mechanisms in Subsection 2.2, the high-Q magnetic resonant coupling provides the best transfer performance of system. In some applications, however, the low-Q magnetic coupling system has its own advantages. As seen from Fig. 7 which shows the comparison between three kinds of coupling, despite the lower efficiency, the low-Q coupling mechanism operates in a wide range of frequency rather than the high-Q coupling. That is why the low-Q factor can be used to detect any possible incoming power. An adaptive Q-tuning circuit is illustrated in Fig. 14. There is no added capacitor in the power coil to set the expected frequency. Actually, the power coil inductively couples with the transmitting coil. Regarding the power coil,  $L_1$  has a number of turns  $N_1$  and  $L'_1$  with  $N'_1$ . These coil turns are connected together by a switch which is implemented by a power MOSFET  $M_1$ . As same as the previous explanation in Subsection 3.1, a current sensor and a differential amplifier are used. In case of the detection of either an absence of any receivers or multiple of them, the sensed current is low causing a small value of  $V_d$ . This value is then compared with a reference voltage  $V_{ref}$  by a comparator. Because of the lower value of  $V_d$  than  $V_{ref}$ , the output of the comparator is set to low, which makes the switch  $M_1$  turn on while  $M_2$  turn off. By the way, the number of coils turns increase by  $N'_1$ , which reduces the quality factor  $Q$  of the transmitting resonator due to a lower turns ratio between the power coil and the transmitting coil (Cannon et al., 2009). On the other hand, in case of one to one system, the switch of  $M_1$  is degenerated while  $M_2$  is activated providing a higher turns ratio which raises the  $Q$  factor of the resonator.

## 4. Conclusion

A general and insightful analysis of WPT system based on electromagnetic resonance is presented. Frequency splitting phenomenon is demonstrated by theoretical derivations

and simulation results as well. Besides, the comparison between different kinds of coupling and case of multiple receivers are also analyzed to impress the need for adaptive circuits to maintain the high performance of the system. Called Antenna- Locked Loops, these circuits offer practical possibilities of WPT with any physical changes. With the wireless power know-how, it is able to counter the transmission of power over distances about tens of feet, although ideally it is very less but still it is impressive. The most interesting fact is that the wireless power transmission is omni directional in nature. If the technology is enhanced and sharpened to be a datum where it can be "generative", it will be able to remain firm to turn the interest of an infinite number of industries. Although, nowadays wireless power is a major obstacle in terms of advancement in the retail sector and also there are many issues regarding the safety, applying and affordability in attentiveness to WPT, but this will likely to be enhanced as the technology further grows up. Generally, this work lays down the ground work of innovative wireless power technology and open opportunities to commercially implement advanced electromagnetic resonance based WPT systems.

## 5. Acknowledgment

This work was supported by Basic Science Research Program through the National Research Foundation of Korea (NRF) funded by the Ministry of Education, Science and Technology (grant number 20110005518).

## 6. References

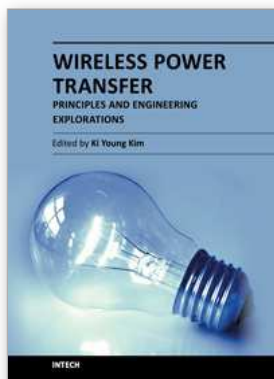
- Brown, W. C. & Eves, E. E. (1992). Beamed Microwave Power Transmission and its Application to Space. *IEEE Transaction on Microwave Theory and Techniques*, vol. 40, no. 6, pp. 1239-1250
- Cannon, B. L.; Hoburg, J.F.; Stancil, D.D. & Goldstein, S.C. (July 2009). Magnetic Resonant Coupling As a Potential Means for Wireless Power Transfer to Multiple Small Receivers. *Power Electronics, IEEE Transactions on*, vol.24, no.7, pp.1819-1825
- Chen, C.J.; Chu, T.H.; Lin, C.L. & Jou, Z.C. (July 2010). A Study of Loosely Coupled Coils for Wireless Power Transfer. *Circuits and Systems II: Express Briefs, IEEE Transactions on*, vol. 57, no.7, pp.536-540
- Greene, C. E; Harrist, D. W.; Shearer, J. G.; Migliuolo, M. & Puschnigg, G. W. (2007). Implementation of an RF Power Transmission and Network. *International Patent Application*, WO/2007/095267
- IEEE-SA Standards Board (1999). IEEE Standard for Safety Levels with Respect to Human Exposure to Radio Frequency Electromagnetic Fields, 3 kHz to 300 GHz. *IEEE Std. C95.1*
- Imura, T. & Hori, Y. (2011). Maximizing Air Gap and Efficiency of Magnetic Resonant Coupling for Wireless Power Transfer Using Equivalent Circuit and Neumann Formula. *Industrial Electronics, IEEE Transactions on*, vol. 58, no. 10, pp. 4746-4752
- Karalis, A.; Joannopoulos, J.D. & Soljacic, M. (January 2008). Efficient Wireless Non-radiative Mid-range Energy Transfer. *Annals of Physics*, vol. 323. No. 1, pp.34-48

Sample, A. P.; Meyer, D.A. & Smith, J.R. (February 2011). Analysis, Experimental Results, and Range Adaptation of Magnetically Coupled Resonators for Wireless Power Transfer. *Industrial Electronics, IEEE Transactions on* , vol.58, no.2, pp.544-554

Tesla, Nikola (1919). The True Wireless. *Electrical Experimenter*, USA

INTECH

INTECH



## **Wireless Power Transfer - Principles and Engineering Explorations**

Edited by Dr. Ki Young Kim

ISBN 978-953-307-874-8

Hard cover, 272 pages

**Publisher** InTech

**Published online** 25, January, 2012

**Published in print edition** January, 2012

The title of this book, *Wireless Power Transfer: Principles and Engineering Explorations*, encompasses theory and engineering technology, which are of interest for diverse classes of wireless power transfer. This book is a collection of contemporary research and developments in the area of wireless power transfer technology. It consists of 13 chapters that focus on interesting topics of wireless power links, and several system issues in which analytical methodologies, numerical simulation techniques, measurement techniques and methods, and applicable examples are investigated.

### **How to reference**

In order to correctly reference this scholarly work, feel free to copy and paste the following:

Huy Hoang and Franklin Bien (2012). Maximizing Efficiency of Electromagnetic Resonance Wireless Power Transmission Systems with Adaptive Circuits, *Wireless Power Transfer - Principles and Engineering Explorations*, Dr. Ki Young Kim (Ed.), ISBN: 978-953-307-874-8, InTech, Available from: <http://www.intechopen.com/books/wireless-power-transfer-principles-and-engineering-explorations/maximizing-efficiency-of-electromagnetic-resonance-wireless-power-transmission-systems-with-adaptive>

**INTeCH**  
open science | open minds

### **InTech Europe**

University Campus STeP Ri  
Slavka Krautzeka 83/A  
51000 Rijeka, Croatia  
Phone: +385 (51) 770 447  
Fax: +385 (51) 686 166  
[www.intechopen.com](http://www.intechopen.com)

### **InTech China**

Unit 405, Office Block, Hotel Equatorial Shanghai  
No.65, Yan An Road (West), Shanghai, 200040, China  
中国上海市延安西路65号上海国际贵都大饭店办公楼405单元  
Phone: +86-21-62489820  
Fax: +86-21-62489821